

1 **Respiratory syncytial virus activates Rab5a to suppress IRF1-dependent IFN- λ**
2 **production, subverting the antiviral defense of airway epithelial cells**

3 Leiqiong Gao¹, Wei Tang¹, Jun Xie¹, Sisi Chen¹, Luo Ren¹, Na Zang² Xiaohong Xie², Yu
4 Deng², Enmei Liu^{2#}

5
6 ¹Pediatric Research Institute, Ministry of Education Key Laboratory of Child
7 Development and Disorders, Key Laboratory of Pediatrics in Chongqing,
8 CSTC2009CA5002, Chongqing International Science and Technology Cooperation Center
9 for Child Development and Disorders, Chongqing 400014, China

10
11 ²Department of Respiratory Medicine, Children's Hospital, Chongqing Medical
12 University, Chongqing 400014, China.

13 Key words: Respiratory syncytial virus; Ras-related protein 5a; Interferon regulatory
14 factor 1; Interferon lambda; Antiviral defense.

15 Running Title: Rab5a subverts the antiviral defense of airway epithelial cells

16

17 **Corresponding author:**

18 Enmei Liu, MD, PhD

19 Department of Respiratory Medicine Children's Hospital of Chongqing Medical
20 University

21 Chongqing, China, 400014

22 Tel: +08613368070773

23 Fax: 086-02363633054

24 E-mail: emliu186@126.com

25

26

27

28

29 **Abstract**

30 Human respiratory syncytial virus (RSV) is a negative-strand RNA virus that causes severe
31 acute pediatric respiratory tract infections worldwide. The limited effective antiviral
32 options and lack of an effective vaccine against RSV highlight the need for a novel anti-
33 viral therapy. One alternative is to identify and target the host factors required for viral
34 infection. All viruses, including RSV, utilize cellular trafficking machinery to fulfill their
35 life cycle in the infected host cells. Rab proteins mediate specific steps in intracellular
36 membrane trafficking through the recruitment and tethering of fusion factors, and docking
37 with actin- or microtubule-based motor proteins. Using RNA interference to knock down
38 Rab proteins, we document that the micropinocytosis-associated Rab5a is required for RSV
39 infection. RSV infection itself induces activation of Rab5a, and inhibition of this activation
40 reduces RSV infection, but the mechanism for this effect remains unknown. Interferon
41 (IFN) signaling plays an important role in innate immunity, and recent studies have
42 identified IFN- λ (lambda), a type III IFN, as the most important IFN for antiviral immune
43 in response to RSV infection of mucosal epithelium. However, how the RSV-induced
44 Rab5a suppresses airway epithelial antiviral immunity has not been unraveled. Here, we
45 show that activated Rab5a inhibits IRF1-induced IFN- λ production and IFN- λ -mediated
46 signal transduction via JAK-STAT1, thereby increasing viral replication. Rab5a
47 knockdown by siRNA resulted in stimulation of IRF1, IFN- λ and JAK-STAT1 expression,

48 and suppressed viral growth. Our results highlight new role for Rab5a in RSV infection,
49 such that its depletion inhibits RSV infection by stimulating the endogenous respiratory
50 epithelial antiviral immunity, which suggests that Rab5a is a potential target for novel
51 therapeutics against RSV infection.

52 **Author summary**

53 RSV is the leading cause of lower respiratory tract infection in under 5 years old children.
54 Worldwide. We identified Rab5a as a host factor involved in RSV infection via RNA
55 interference to knock down familiar Rab proteins in human lung epithelial A549 cells
56 infected with RSV. Rab5a belongs to Rab GTPases subfamily, which contributes to
57 intracellular trafficking to promote virus infection. Knockdown or inactive (GDP-bound)
58 Rab5a results in low infection and replication through stimulating IRF1, IFN- λ and JAK-
59 STAT1 expression, and suppressed viral growth. Besides, we propose that the regulation
60 of Rab5a expression during RSV infection might be a viral strategy to promote its
61 infectivity.

62

63

64

65

66

68 **Introduction**

69 Human respiratory syncytial virus (RSV) belongs to the *Paramyxoviridae* family [1],
70 and is a leading cause of respiratory tract infection in young children [2]. Approximately 4
71 million children worldwide are admitted to hospitals each year with RSV infection, 3.4
72 million of whom develop severe symptoms such as bronchiolitis and pneumonia [3-5]. The
73 healthcare costs of hospitalization from the RSV-infected patients are significant [6,7], and
74 despite years of ongoing efforts, there is currently no safe or effective vaccine available to
75 protect children and minimize the global burden of RSV. Thus, identification of host
76 factors required for RSV infection may be considered as a plausible alternative to develop
77 a therapeutic regimen.

78 Being obligatory intracellular parasites, viruses utilize diverse cellular trafficking
79 machinery to achieve productive life cycles in the infected host cells. Members of the Rab
80 family of cellular proteins regulate actin- or microtubule-based motor proteins and
81 intracellular membrane trafficking, and have been implicated in various steps of the viral
82 life cycle, including replication, assembly, and budding. To identify cellular Rab proteins
83 required for RSV infection, we interrogated the role of nine widely expressed Rab proteins
84 (Rab1a, Rab2a, Rab4a, Rab5a, Rab6a, Rab7a, Rab8a, Rab9a, Rab11a) that are involved in
85 the endo- or exocytic pathways. Using specific siRNA to knock down each Rab protein,
86 we found that the micropinocytosis-associated Rab5a protein is required for RSV infection,
87 which confirmed and extended our previous iTRAQ data suggesting this role of Rab5a

88 (unpublished data). Additionally, RSV infection activated Rab5a, which is related to actin-
89 mediated micropinocytosis of RSV, and recent studies showed that inhibition of Rab5a
90 results in decreased RSV titers [8]. In another study, depletion of Rab5a by siRNA resulted
91 in decreased RSV replication, but viral binding was not affected [9]. Together, these
92 findings further suggested that inhibition of Rab5a activation affects post-entry steps of the
93 viral life cycle.

94 Rab5a, a major member of the small GTPase Rab family, is mainly localized to the
95 cytosolic face of the plasma membrane, early endosomes, clathrin-coated vesicles and
96 macropinosomes [10-13]. The Rab5a activity depends on GDP/GTP association [14]; the
97 activity is also spatially regulated and ensure the bi-directionality of the processes it
98 governs. Several studies have demonstrated that Rab5a, in particular, plays a critical role
99 in viral infection. For example, components of positive-strand RNA viral replication can
100 hijack Rab5a to promote viral replication [15]; the influenza A virus uses Rab5a to
101 modulate Annexin-A1, thus enhancing its replication [16]; HIV and hepatitis B/C viruses
102 co-opt Rab5a to enter cells [17-21]. The involvement of Rab5a in RSV endocytosis or
103 micropinocytosis has been described previously [8], and as mentioned above, knockdown
104 of Rab5a resulted in decreased RSV replication [9]. In parallel, several studies
105 demonstrated that Rab5a is closely related to innate immunity. IFN-gamma (IFN- γ), a type
106 II interferon, induces Rab5a synthesis [22-24], which acts to mediate the bactericidal effect
107 of IFN- γ . In addition, IL-4 and -6 increase Rab5 expression [25], and IL-4 also extends the

108 retention of Rab5 on phagosomes in a PI3K-dependent manner [26]. Rab5a is closely
109 related to the IFN-signaling JAK-STAT pathway, and downregulation of Rab5a increases
110 STAT1 expression [27,28]. Rab5a also affects TLR4-mediated innate immunity [29].
111 Rab5a is required for the formation of the early endosome, which is related to the IFN-
112 induced transmembrane proteins of the IFITM family; moreover, the type I IFN receptor
113 complex is also differentially sorted at the early endosome [30]. Taken together, these
114 studies suggest that Rab5a may affect the innate immunity in RSV infection. Lastly, several
115 RNA viral nonstructural proteins, such as the NS proteins of RSV, subvert IFNs, and Rab5
116 has been shown to co-localize with NS-induced structures of the SFTS (Severe fever with
117 thrombocytopenia syndrome) virus [31]. Based on these findings, we hypothesize that
118 Rab5a facilitates RSV infection, not because it promotes virion binding, but because it
119 inhibits the cell-intrinsic antiviral IFN pathway. Nonetheless, there are currently no studies
120 of the effect of Rab5a on IFN signaling.

121 As mentioned, IFN signaling is a major arm of the innate antiviral response of the host.
122 Recent studies revealed that that IFN- λ , a type III IFN, is also an important IFN of the
123 airway epithelium [32,33]. Further studies suggested that type I IFNs (i.e., IFN- α and IFN- β)
124 are critical for the clearance of infection, whereas IFN- λ is the most important IFN
125 regulating mucosal epithelial cell responses to viral infection [33,34]. Recent studies of the
126 Koff group found that IFN- λ is the first produced IFN of the RSV-exposed nasal epithelium
127 [35]. Moreover, RSV could inhibit IFN- λ production in lung epithelial cells, and IFN- λ

128 was critical for antiviral immunity to RSV [36,37]. Further studies suggested that RSV
129 induces IFN- λ production by activating IRF1, a transcription factor for the IFN- λ gene
130 [35]. However, the potential role for Rab5a pathway in modulating IFN- λ and its related
131 innate immunity in RSV infection has not been reported. Here, we have explored the effect
132 of the Rab5a pathway on RSV infection in airway epithelial cells and the role of IFN- λ -
133 related factors in this process. We show that RSV infection indeed activates Rab5a, which
134 in turn facilitates viral infection by regulating the pathways related to IFN- λ .

135

136

137

138

139

140

141

142

143

144

145

146 **Results**

147 **Rab5a is essential for RSV production**

148 Studies in this section interrogated the effect of Rab5a on RSV infection in airway
149 epithelial A549 cells. To this end, we depleted Rab1a, Rab2a, Rab4a, Rab5a, Rab6a, Rab7a,
150 Rab8a, Rab9a and Rab11a by treating the cells with specific siRNAs (or control siRNA)
151 for 24 h p.i., followed by infection with purified RSV A2 and incubation for another 36 h.
152 Depletion of Rab proteins was confirmed by immunoblotting analysis of the total cell
153 lysates (Figure 1B). To determine the viral load, the viral N gene RNA was quantified by
154 RT-qPCR on RNA isolated at 36 h p.i. (Figure 1C). The syncytial area and number were
155 counted using Image J (Figure 1A & 1D). Little alteration of RSV replication was observed
156 following depletion of Rab1a, Rab2a and Rab6a compared to the control cells treated with
157 siRNA (Figures 1A and 1C). A moderate decrease in RSV replication was observed on
158 knockdown of Rab4a, Rab7a, Rab8a and Rab9a, with 40-70% less N gene detected both in
159 the cells and supernatant compared to the control. The effects of Rab11a depletion were
160 similar to those reported previously [38,39]. The most potent effect on RSV propagation
161 was observed in cells depleted of Rab5a. Indeed, after 48 h p.i., only a few infected cells
162 were observed in Rab5a-depleted cultures (Figure 1A & 1D) and the level of N was more
163 than 30-fold lower than the control (Figure 1C). These results suggest that Rab5a plays an
164 important role in RSV propagation.

165 **RSV infection increases Rab5a expression**

166 To investigate the induction of Rab5a by RSV in the infected cells, we measured total
167 Rab5a mRNA and protein by RT-qPCR and immunoblotting at various post-infection
168 times. It was observed that both Rab5a mRNA and Rab5a protein levels significantly
169 increased starting at 1 h p.i. (Fig. 1), when compared with mock infection. These results
170 confirmed that RSV indeed induces Rab5a expression.

171 **Rab5a-GTP active form required for RSV infection**

172 To examine whether Rab5a-GTP affects RSV replication, recombinant EGFP-Rab5a (wild
173 type), constitutively active (C/A) mutant, Q79L, and the dominant negative (D/N) mutant,
174 S34N, were transiently transfected in A549 cells. Q79L can enlarge Rab5a-positive
175 vacuoles, but fails to undergo further maturation[40]. S34N inhibits Rab5a-GDP transfer
176 to Rab5a-GTP, and thus inhibits Rab5a located on the membrane[41]. After 24 h
177 transfection, cells were infected with RSV for the indicated time. Viral load analysis
178 demonstrated that S34N was the only one that caused a significant decrease in RSV
179 infection when overexpressed (Fig. 3B). These results confirm and extend those reported
180 by the Helenius laboratory [8]. Consistent with the viral load results, we also found that
181 Q79L showed higher co-localization with RSV compared to EGFP-Rab5a cells by using
182 confocal microscopy. In contrast, EGFP-Rab5a S34N showed the lowest amount of virus
183 particles and least co-localization among the three groups (Fig. 3A). However, no
184 significant changes were observed in cells expressing EGFP-Rab5a. Together, these results
185 confirmed that the active form of Rab5a is in fact essential for RSV replication in vitro.

186 **Rab5a depletion exaggerates epithelial antiviral defense to RSV**

187 No mechanism for Rab5a-mediated enhancement of RSV growth has yet been reported.

188 To explore this mechanism, we evaluated the effect of Rab5a signaling on airway epithelial
189 antiviral innate immunity. Type I and Type III IFN play an important role in innate and
190 adaptive antiviral immunity. As indicated earlier, recent studies have implicated that
191 besides IFN- α and IFN- β , IFN- λ is another important IFN that responses to RSV infection
192 in the respiratory epithelia. We, therefore, focused on the potential role for Rab5a in
193 regulating the production of all three IFNs. A549 cells were transfected with siRNAs
194 specific for Rab5a (and siRNA control) for 24 h, and infected with RSV for another 24 h
195 p.i.. Control, mock-infected cells received the same volume of media. Results show that
196 RSV could indeed induce IFN- α (Fig. 4A & 4B), IFN- β (Fig. 4C & 4D) and IFN- λ (Fig.
197 4E & 4F), when compared with mock infection. Rab5a depletion further increased IFN- λ
198 production significantly (Fig. 4E & 4F), and slightly increased IFN- α and IFN- β production,
199 compared to siCON in RSV-infected cells (Fig. 4A & 4D). The Rab5a S34N mutant also
200 enhanced IFN- λ production (Fig. 4G). These data suggest that during RSV infection Rab5a
201 inhibition increased IFN- λ production.

202 The IFN regulatory factors (IRFs), functioning as transcription factors, play an important
203 role in IFN production. RSV can activate IRF1 in monocytes and lung epithelial
204 cells[42,43], and the IRF1 can interact with the IFN- λ promoter to induce IFN- λ
205 transcription. Thus, to explore the effect of Rab5a on IRF1 expression during RSV

206 infection, we transfected siRab5a and siCON into A549 cells for 24 h, and then infected
207 with RSV for another 24 h. Interestingly, we found that RSV infection increased IRF1
208 levels, and depletion of Rab5a further increased IRF1 expression during RSV infection
209 (Fig. 5A & 5B). The immunofluorescence staining confirmed these data (Fig. 5C & 5D).
210 Overall, these results suggested that depletion of Rab5a increased IRF1 expression.

211 To confirm the important role of IRF1 in RSV-induced IFN- λ production in epithelial cells,
212 we treated A549 cells with IRF1-specific siRNA, which significantly suppressed IRF1
213 protein levels (Fig. 6A). Treatment with this siIRF1 decreased the expression of IFN- λ
214 production in RSV-infected A549 cells, when compared with cells infected with RSV but
215 treated with control siRNA (Fig. 6B). Moreover, siIRF1 eliminated the effect of siRab5a
216 in exaggerating IFN- λ production (Fig. 6C) that we showed earlier (Fig. 4E). Together,
217 these results suggest that: (i) depletion of IRF1 reduces IFN- λ production; (ii) siRab5a
218 exaggerates IFN- λ production via IRF1.

219 **Rab5a depletion leads to an increase of STAT1**

220 IFN- λ binds to its unique receptor complex (IFN-IR1/IL-10R2), which triggers a signaling
221 cascade by activating the downstream JAK-STAT pathway, among which the JAK-STAT1
222 pathway plays an important role in response to RSV infection. To investigate the effect of
223 Rab5a depletion on JAK-STAT1, A549 cells were transfected with Rab5a-specific siRNA
224 (or control siRNA) for 24 h p.i., then infected with RSV for as before. STAT1 expression
225 was then quantified by immunoblotting. Results (Fig. 7) revealed that RSV infection

226 increased STAT1, and Rab5a depletion increased it further, which lead to an increase in
227 both total STAT1 (Fig. 7AB) and phosphorylated STAT1 species (p-STAT1) (Fig. A,C,D).
228 Moreover, the addition of a JAK1 or STAT1 inhibitor abrogated the ability of siRab5a to
229 suppress RSV infection (Fig. 7D). These results demonstrate that IFN- λ -induced JAK-
230 STAT1 signaling accounts for the effect of IFN- λ on siRab5a-mediated inhibition of RSV.

231 **Rab5a depletion amplifies RIG-I and Mx1 expression, in part via the JAK-STAT1**
232 **pathway**

233 Previous studies found that RSV infection induces RIG-I and Mx1 production[44,45].
234 RIG-I and Mx1 are downstream genes of the JAK-STAT1-dependent IFN response
235 pathway. We first confirmed this induction, and showed that depletion of Rab5a indeed
236 increased the expression of these two genes (Fig.8A & 8C). Inhibition of JAK and STAT1
237 by specific inhibitors, Baricitinb and Fludarabine respectively, partially rescued this
238 increase of RIG-I and Mx1 (Fig. 7B & 7D), suggesting that the induction of RIG-I and
239 Mx1 by Rab5a occurs via the JAK-STAT pathway.

240

241

242

243

244

245 **Discussion**

246 Results presented here support an important role of Rab5a in RSV replication. RSV
247 infection increased the amount of Rab5a in airway epithelial cells. The biological effect of
248 this increased Rab5a is to suppress host anti-viral immunity (Fig. 9A). Knockdown of
249 Rab5a gene expression or its inhibition by dominant negative mutants in A549 cells results
250 in protection against RSV infection through the activation of IRF1-dependent, IFN- λ
251 mediated anti-viral pathway (Fig. 9B). Indeed, the presence of Rab5a leads to higher
252 infection and replication of the virus. This study is the first to show that in airway epithelial
253 cells: (i) RSV infection alters the amount of Rab5a, (ii) Rab5a enhances RSV replication,
254 (iii) the mechanism of this effect of Rab5a involves regulation of IRF1, IFN- λ and STAT1,
255 and (iv) Rab5a may thus attenuate inflammation of the epithelia during RSV infection.

256 While previous studies have demonstrated an effect of Rab5a in diverse virus replication
257 [18,21,46], none have shown an alteration of Rab5a protein levels in RSV infection.
258 Krzyzaniak et al found that inhibiting the activation of Rab5a attenuates viral titer in RSV
259 infection of HeLa cells [8]. Another study, mentioned earlier, found that depletion of Rab5a
260 resulted in decreased RSV replication, and viral binding was not affected when suppressed
261 action of Rab5a [9]. We confirmed and extended these studies and found that there is no
262 significant difference of viral binding between Rab5a-depleted and untreated cells (Fig.
263 S3). Together, these results establish that depletion of Rab5a has no effect on RSV binding
264 to airway epithelial cells.

265 Rab5a is also required for macrosome formation. Previous studies suggested that RSV
266 entry into host cell takes place via actin-related micropinocytosis [8]. In the very first step
267 of RSV infection, the virions need to engage cellular receptors to trigger entry into the cell.
268 Studies have suggested a plethora of candidate cellular receptors for RSV entry, for
269 example, CX3CR [47-49], EGFR [50,51], TLR4 [52,53], ICAM-1 [54], nucleolin [55,56],
270 and HSPGs [57]. Among these, EGFR plays a particularly important role in RSV infection
271 and inflammation [58], and the mechanism is related to IRF1-dependent IFN- λ [35].
272 Multiple studies have shown that EGFR closely interacts with Rab5a. For example, Rab5a
273 is very important for EGFR trafficking, and endogenous EGFRs can partially co-localize
274 with endogenous Rab5 [59]. Stahl [60] reported that EGFR stimulates the activation of
275 Rab5a, and also enhances the translocation of Rab5a. Meanwhile, suppression of Rab5a
276 hampered the degradation of EGFR and its internalization. Furthermore, Rab5a
277 overexpression facilitated cell proliferation through the EGFR signal pathway [61]. In our
278 studies, RSV infection activated not only Rab5a (Fig. 2), but also EGFR (unpublished data).
279 Depletion of Rab5a decreased the activation of EGFR, and inhibition of EGFR by Gefitinib
280 also suppressed Rab5a protein level; finally, both Rab5a depletion and Gefitinib treatment
281 decrease RSV infection via IRF1-dependent IFN- λ production [35]. Altogether, our
282 current studies predict that Rab5a may promote viral infection through EGFR, further
283 investigation is needed to determine how exactly Rab5a and EGFR influence each other
284 during RSV infection.

285 The nonstructural proteins (NS1 and NS2) of RSV suppress host innate and adaptive
286 immune responses against the virus. Both proteins, individually and in combination, inhibit
287 type I IFN pathway [62], and the NS1 protein also suppresses IFN- λ production in airway
288 epithelial cells during RSV infection [37]. In our study, depletion of Rab5a amplified IFN- λ
289 production in RSV infection, moreover, overexpression of Rab5a increased NS1 mRNA
290 and protein level (data not shown). Therefore, our data predicted that Rab5a also may
291 promote RSV NS1 production to anti-epithelial antiviral defenses. We need further
292 investigate the correlation between Rab5a and RSV NS1.

293 Lastly, we have documented that inhibition of Rab5a needed IRF1 and IFN- λ to restrain
294 RSV infection, and the JAK-STAT1 pathway was implicated in this effect. In agreement
295 with a previous study [35], we also found that exogenously added recombinant IFN- λ could
296 inhibit RSV infection, which demonstrate an important antiviral role of this pathway,
297 defending the airway epithelial cells against RSV. However, the mechanism by which
298 Rab5a suppresses IRF1 still needs to be elucidated. Another study found that ERK
299 inhibition could increase RSV-induced IFN- λ production [35]. Therefore, we need further
300 investigate whether ERK signaling may act as a critical link in the mechanism connecting
301 IRF1 and Rab5a.

302 In conclusion, although limited in scope, our studies have demonstrated that Rab5a plays
303 an important role in RSV infection. We have also discovered a new mechanism in which
304 RSV uses Rab5a to suppress epithelial antiviral immunity, such that silencing or

305 inactivating Rab5a results in reduced viral infection. This is a new insight on the role of
306 the cellular factor Rab5a in RSV infection, which can be explored as a therapeutic and
307 druggable target against RSV infection.

308

309

310

311

312

313

314

315

316

317

318

319

320

321

322

323 **Materials and Methods**

324 **Research subjects**

325 Twenty-six children with RSV infection, hospitalized from November 2016 to January
326 2017 in the Department of Respiratory Medicine, Children's Hospital, Chongqing Medical
327 University, were enrolled in this study. Nasopharyngeal aspirates (NPAs) were
328 prospectively collected from all subjects within the first day after hospital admission.
329 Immunofluorescence assays were performed to detect the presence of RSV, adenovirus,
330 influenza A and B virus, and parainfluenza virus 1, 2, and 3 in the NPAs. Infants that
331 carried viruses other than RSV were excluded from the study. Those considered positive
332 for bacterial infection on the basis of published criteria [63] were excluded as well. The
333 control group was selected from infants with no evidence of infection, and underwent
334 surgical therapy only to clear secretions from the airway.

335 **Nasopharyngeal aspirate analysis**

336 NPAs were collected and analyzed as previously described [63]. In brief, they were
337 collected gently and mixed uniformly. To 0.5 mL of the aspirate, transferred to a new tube,
338 2 mL of 0.1% dithiothreitol was added. The mixture was vortexed three times, 15 seconds
339 each, and rocked on a bench rocker for 15 min. The suspension was collected and
340 subsequently centrifuged at 306 g for 10 min. Cell-free supernatants were collected and
341 aliquots stored at -80°C . The cell pellet was used for total RNA and protein extraction.

342 **Reagents, antibodies and plasmids**

343 The primary antibodies used in this study include a goat polyclonal antibody to RSV,
344 purchased from Millipore, and rabbit Rab (Rab1a, Rab2a, Rab4a, Rab5a, Rab6a, Rab7a,
345 Rab8a, Rab9a and Rab11a), STAT1, phospho-STAT1 (Tyr701), IRF1, and mouse GAPDH
346 monoclonal antibodies, purchased from Cell Signaling Technology (CST), USA. DAPI

347 was purchased from Sigma-Aldrich, USA. The secondary antibodies used were Alexa
348 Fluor 568/488-conjugated duck anti-goat IgG or anti-rabbit IgG from Biyuntian, Beijing,
349 China, and horseradish peroxidase (HRP)-conjugated goat anti-rabbit IgG or anti-mouse
350 IgG from CST, USA. Expression plasmids encoding EGFP-tagged Rab5a and its mutants
351 were purchased from Addgene, USA. The Janus kinase 1 (JAK1) inhibitor, Baricitinib,
352 was purchased from MedChemExpress, Shanghai, China, and the STAT1 inhibitor,
353 Fludarabine, from Selleckchem.

354 **Cell culture, virus and infection**

355 Human alveolar carcinoma type II-like epithelial cell line A549 (ATCC CCL-185) and
356 human laryngeal cancer epithelial cell line HEp-2 (ATCC CCL-23) were cultured in
357 Dulbecco's Modified Eagle Medium (DMEM) supplemented with 10% fetal bovine. RSV
358 A2 strain was obtained from ATCC. For all experiments, RSV was grown in HEp-2 cells
359 with 5% FBS and purified by density gradient as previously described [64]. In all
360 experiments where RSV infection was performed, a multiplicity of infection (MOI) of 0.8
361 was used.

362 **Virus titration**

363 At indicated times, the infected cell media supernatants were collected, and the cells were
364 scraped into the cell culture medium and vortexed three times with glass beads, followed
365 by centrifugation at 1000 rpm for 5 min. RSV titration was performed by plaque assay on
366 HEp-2 cells.

367 **siRNA transfection**

368 The Rab (Rab1a, Rab4a, Rab5a, Rab6a, Rab7a, Rab8a, Rab9a and Rab11a) siRNA
369 sequences were from reference [65], and were as follows. The Rab1a siRNAs:
370 5'CAGCAUGAAUCCCGAAUAU; 5'GUAGAACAGUCUUUCAUGA; 5'
371 GUAGAACAGUCUUUCAUGA; 5'UGAGAAGUCCAAUGUUAAA; Rab4a
372 siRNAs :5'GAAAGAAUGGGCUCAGGUA; 5'GUU AACAGAUGCCCGAAUG;
373 5'UUAGAAGCCUCCAGAUUUG; 5'UACAAUGCGCUUACUAAUU; Rab5a siRNAs:
374 5'GCAAGCAAGUCCUAACAUU; 5'GGAAGAGGAGUAGACCUUA;
375 5'AGGAAUCAGUGUUGUAGUA; 5'GAAGAGGAGUAGACCUUAC; Rab6a siRNA:
376 5'GAGAAGAU AUGAUUGACAU; 5'GAGCAACCAGUCAGUGAAG;
377 5'AAGCAGAGAAGAU AUGAUU; 5'CAAAGAGCUGAAUGUUUU; Rab7a siRNA:
378 5'GGGAGUUCUGGAGUCGGGAA; 5'CCACAAUAGGAGCUGACUU3'. Rab8a
379 siRNAs: 5'GAAUUAAACUGCAGAU AUG; 5'GAACAAGUGUGAUGUGAAU;
380 5'GAACUGGAUUCGCAACA UU; 5'GAAGACCUGUGUCCUGUUC; Rab9a siRNA
381 duplex: 5'CGGCAGGTGTCTACAGAAG; Rab11A siRNAs:
382 5'GGAGUAGAGUUUGCAACAA; 5'GUAGGUGCCUUAUUGGUUU;
383 5'GCAACAAUGUGGUUCCUAU; 5'CAAGAGCGAU AU CGAGCUA. These and the
384 IRF1 siRNA (duplex UCCCAAGACGUGGAAGGCCAACUUU) were purchased from
385 Qiagen. The siRNA against human Rab2a was purchase from Sigma Aldrich. Cell lysates
386 were separated by SDS-PAGE and subjected to immunoblotting with rabbit anti-Rabs,

387 rabbit anti-IRF1, or mouse anti-GAPDH (as a loading control) antibodies.

388 **Immunoblotting**

389 Total cell protein (50 µg) was resolved on 5-15% Bis-tris SDS-PAGE, and transferred onto
390 PVDF membranes. The membranes were incubated with primary antibodies against Rab
391 proteins, IRF1, GAPDH, or LaminB1, followed by incubation with appropriate secondary
392 antibodies. The protein bands were visualized with a chemiluminescence kit (Bio-Rad).

393 **Quantitative (q) RT-PCR**

394 A549 cells, transfected with plasmids, and infected with RSV as and where mentioned,
395 were harvested, and intracellular RNA was purified at indicated times post-transfection
396 (BioTake). Viral RNA was isolated from the Mixture of cells and media supernatants. The
397 RNA (1 µg) was used for first-strand cDNA synthesis and the cDNA was amplified using
398 the VeriQuest Fast SYBR Green qPCR kit (Invitrogen) with primers as follows: Rab5a
399 (forward primer 5' CAAGAACGATACCATAGCCTAGCAC3'; reverse primer 5'
400 CTTGCCTCTGAAGTTCTTTAACCC 3'); IFNA1 (forward primer 5'
401 GTGAGGAAATACTTCCAAAGAATCAC3'; reverse primer 5'
402 TCTCATGATTTCTGCTCTGACAA 3'); IFNB1 (forward primer 5'
403 CAGCAATTTTCAGTGTGTCAGAAGC3'; reverse primer 5'
404 TCATCCTGTCCTTGAGGCAGT 3'); IFN-λ(forward primer 5'
405 CGCCTTGGAAGAGTCACTCA3'; reverse primer 5'
406 GAAGCCTCAGGTCCCAATTC3').

407 RSV copy numbers were quantified with TaqMan RT-PCR as previously described [66].
408 The PCR cycle conditions were as follows: 50°C for 2 min, 95°C for 10 min, 40 cycle at 95°C
409 for 15 s and 60°C for 30 s. The fold change was obtained using 2- $\Delta\Delta C_t$ method using
410 GAPDH as a calibrator.

411 **Transfection and transient expression**

412 All plasmid transfections were performed with a commercial transfection kit (Thermo
413 Fisher Scientific, USA). Cells were seeded on 12 mm coverslips in 24 wells for imaging
414 or in 6-well plates for qRT-PCR or immunoblotting analyses. Experiments were performed
415 at indicated times after transfection.

416 **Indirect immunofluorescence assays**

417 RSV-infected A549 cells were fixed with 4% paraformaldehyde for 30 min at room
418 temperature and permeabilized with 0.2% Triton X-100 (sigma) for an additional 20 min.
419 After washing and blocking with 2% BSA for 1 h, the cells were incubated with anti-IRF1
420 or anti-RSV antibody at 4 °C overnight. The cells were then washed three times, followed
421 by incubation with Alexa Fluor 568-conjugated secondary antibodies (Molecular Probes)
422 for 1 h at room temperature. Finally, the cells were visualized and photographed using a
423 Nikon laser confocal microscope. in which the images were acquired with confocal Z-
424 section series and were subsequently analyzed with NIS-Elements BR software, version
425 4.11.

426 **Syncytia quantification**

427 Quantification of the RSV syncytia was performed as described by Buchholz et al
428 (2016)[67], with minor modifications. A549 cells were grown in three coverslips in 24
429 wells per group, and infected with RSV at MOI 0.8 where mentioned, then fixed at 24 h
430 post-infection (p.i.), and stained with DAPI and for RSV. The three coverslips were imaged
431 and NIS software was used to draw the area of the syncytia. Image J (NIH) was used to
432 confirm the syncytial area. Syncytia were counted when they were RSV-positive.

433 **Measurement of IFN**

434 Human-specific enzyme-linked immunosorbent assay (ELISA) kits were used to measure
435 IFN- α , IFN- β and IFN- λ levels in culture supernatants (BD, USA).

436 **Statistical analysis**

437 Data analysis were performed using SPSS 19.0 software. One-way analysis of variance
438 (ANOVA) was used to detect the significance of the difference among groups. Unpaired
439 Student's t-test was used to detect the significance between two groups. *P* value of < 0.05
440 was considered significant.

441 **Ethics Statement**

442 Use of NPA samples of infants were approved by the Ethics Committee of the Children's
443 Hospital, Chongqing Medical University (permit number 2015-77). The parents or legal
444 guardians offered written informed consent to participate in the study before the infants
445 were enrolled. All procedures were performed in accordance with the approved guidelines,
446 and obeyed the principles of the Declaration of Helsinki.

447

448

449 Reference

- 450 1. Afonso CL, Amarasinghe GK (2016) Taxonomy of the order Mononegavirales: update 2016. *161*: 2351-
451 2360.
- 452 2. (!!! INVALID CITATION !!!).
- 453 3. Nair H, Nokes DJ, Gessner BD, Dherani M, Madhi SA, et al. (2010) Global burden of acute lower
454 respiratory infections due to respiratory syncytial virus in young children: a systematic review
455 and meta-analysis. *Lancet* *375*: 1545-1555.
- 456 4. Nair H, Simoes EA, Rudan I, Gessner BD, Azziz-Baumgartner E, et al. (2013) Global and regional burden
457 of hospital admissions for severe acute lower respiratory infections in young children in 2010: a
458 systematic analysis. *Lancet* *381*: 1380-1390.
- 459 5. Byington CL, Wilkes J, Korgenski K, Sheng X (2015) Respiratory syncytial virus-associated mortality in
460 hospitalized infants and young children. *Pediatrics* *135*: e24-31.
- 461 6. Langley JM, Wang EE, Law BJ, Stephens D, Boucher FD, et al. (1997) Economic evaluation of respiratory
462 syncytial virus infection in Canadian children: a Pediatric Investigators Collaborative Network on
463 Infections in Canada (PICNIC) study. *J Pediatr* *131*: 113-117.
- 464 7. Paramore LC, Ciuryla V, Ciesla G, Liu L (2004) Economic impact of respiratory syncytial virus-related
465 illness in the US: an analysis of national databases. *Pharmacoeconomics* *22*: 275-284.
- 466 8. Krzyzaniak MA, Zumstein MT, Gerez JA, Picotti P, Helenius A (2013) Host cell entry of respiratory
467 syncytial virus involves macropinocytosis followed by proteolytic activation of the F protein. *PLoS*
468 *Pathog* *9*: e1003309.
- 469 9. Ang F, Wong AP, Ng MM, Chu JJ (2010) Small interference RNA profiling reveals the essential role of
470 human membrane trafficking genes in mediating the infectious entry of dengue virus. *Virology* *7*:
471 24.
- 472 10. Bucci C, Parton RG, Mather IH, Stunnenberg H, Simons K, et al. (1992) The small GTPase rab5 functions
473 as a regulatory factor in the early endocytic pathway. *Cell* *70*: 715-728.
- 474 11. Bucci C, Wandinger-Ness A, Lutcke A, Chiariello M, Bruni CB, et al. (1994) Rab5a is a common
475 component of the apical and basolateral endocytic machinery in polarized epithelial cells. *Proc*
476 *Natl Acad Sci U S A* *91*: 5061-5065.
- 477 12. Feliciano WD, Yoshida S, Straight SW, Swanson JA (2011) Coordination of the Rab5 cycle on
478 macropinosomes. *Traffic* *12*: 1911-1922.
- 479 13. Yoshida S, Hoppe AD, Araki N, Swanson JA (2009) Sequential signaling in plasma-membrane domains
480 during macropinosome formation in macrophages. *J Cell Sci* *122*: 3250-3261.
- 481 14. Chavrier P, Parton RG, Hauri HP, Simons K, Zerial M (1990) Localization of low molecular weight GTP
482 binding proteins to exocytic and endocytic compartments. *Cell* *62*: 317-329.
- 483 15. Xu K, Nagy PD (2016) Enrichment of Phosphatidylethanolamine in Viral Replication Compartments via
484 Co-opting the Endosomal Rab5 Small GTPase by a Positive-Strand RNA Virus. *PLoS Biol* *14*:
485 e2000128.

- 486 16. Arora S, Lim W, Bist P, Perumalsamy R, Lukman HM, et al. (2016) Influenza A virus enhances its
487 propagation through the modulation of Annexin-A1 dependent endosomal trafficking and
488 apoptosis. *Cell Death Differ* 23: 1243-1256.
- 489 17. Sheng Y, Li J, Zou C, Wang S, Cao Y, et al. (2014) Downregulation of miR-101-3p by hepatitis B virus
490 promotes proliferation and migration of hepatocellular carcinoma cells by targeting Rab5a. *Arch*
491 *Viro* 159: 2397-2410.
- 492 18. Neil SJ, Eastman SW, Jouvenet N, Bieniasz PD (2006) HIV-1 Vpu promotes release and prevents
493 endocytosis of nascent retrovirus particles from the plasma membrane. *PLoS Pathog* 2: e39.
- 494 19. Berger KL, Cooper JD, Heaton NS, Yoon R, Oakland TE, et al. (2009) Roles for endocytic trafficking and
495 phosphatidylinositol 4-kinase III alpha in hepatitis C virus replication. *Proc Natl Acad Sci U S A*
496 106: 7577-7582.
- 497 20. Collier KE, Berger KL, Heaton NS, Cooper JD, Yoon R, et al. (2009) RNA interference and single particle
498 tracking analysis of hepatitis C virus endocytosis. *PLoS Pathog* 5: e1000702.
- 499 21. Eyre NS, Fiches GN, Aloia AL, Helbig KJ, McCartney EM, et al. (2014) Dynamic imaging of the hepatitis C
500 virus NS5A protein during a productive infection. *J Virol* 88: 3636-3652.
- 501 22. Prada-Delgado A, Carrasco-Marin E, Bokoch GM, Alvarez-Dominguez C (2001) Interferon-gamma
502 listericidal action is mediated by novel Rab5a functions at the phagosomal environment. *J Biol*
503 *Chem* 276: 19059-19065.
- 504 23. Alvarez-Dominguez C, Stahl PD (1998) Interferon-gamma selectively induces Rab5a synthesis and
505 processing in mononuclear cells. *J Biol Chem* 273: 33901-33904.
- 506 24. Pei G, Repnik U, Griffiths G, Gutierrez MG (2014) Identification of an immune-regulated phagosomal
507 Rab cascade in macrophages. *J Cell Sci* 127: 2071-2082.
- 508 25. Wainszelbaum MJ, Proctor BM, Pontow SE, Stahl PD, Barbieri MA (2006) IL4/PGE2 induction of an
509 enlarged early endosomal compartment in mouse macrophages is Rab5-dependent. *Exp Cell Res*
510 312: 2238-2251.
- 511 26. de Keijzer S, Meddens MB, Kilic D, Joosten B, Reinieren-Beeren I, et al. (2011) Interleukin-4 alters early
512 phagosome phenotype by modulating class I PI3K dependent lipid remodeling and protein
513 recruitment. *PLoS One* 6: e22328.
- 514 27. Pereira-Leal JB, Seabra MC (2001) Evolution of the Rab family of small GTP-binding proteins. *J Mol Biol*
515 313: 889-901.
- 516 28. Muller P, Pugazhendhi D, Zeidler MP (2012) Modulation of human JAK-STAT pathway signaling by
517 functionally conserved regulators. *Jakstat* 1: 34-43.
- 518 29. Ghosh M, Subramani J, Rahman MM, Shapiro LH (2015) CD13 restricts TLR4 endocytic signal
519 transduction in inflammation. *J Immunol* 194: 4466-4476.
- 520 30. Chmiest D, Sharma N, Zanin N, Viaris de Lesegno C, Shafaq-Zadah M, et al. (2016) Spatiotemporal
521 control of interferon-induced JAK/STAT signalling and gene transcription by the retromer
522 complex. *Nat Commun* 7.
- 523 31. Santiago FW, Covalada LM, Sanchez-Aparicio MT, Silvas JA, Diaz-Vizarreta AC, et al. (2014) Hijacking of
524 RIG-I Signaling Proteins into Virus-Induced Cytoplasmic Structures Correlates with the Inhibition
525 of Type I Interferon Responses. *J Virol* 88: 4572-4585.
- 526 32. Khaitov MR, Laza-Stanca V, Edwards MR, Walton RP, Rohde G, et al. (2009) Respiratory virus induction

- 527 of alpha-, beta- and lambda-interferons in bronchial epithelial cells and peripheral blood
528 mononuclear cells. *Allergy* 64: 375-386.
- 529 33. Mordstein M, Neugebauer E, Ditt V, Jessen B, Rieger T, et al. (2010) Lambda interferon renders
530 epithelial cells of the respiratory and gastrointestinal tracts resistant to viral infections. *J Virol* 84:
531 5670-5677.
- 532 34. Jewell NA, Cline T, Mertz SE, Smirnov SV, Flano E, et al. (2010) Lambda interferon is the predominant
533 interferon induced by influenza A virus infection in vivo. *J Virol* 84: 11515-11522.
- 534 35. Kalinowski A, Galen BT, Ueki IF, Sun Y, Mulenon A, et al. (2018) Respiratory syncytial virus activates
535 epidermal growth factor receptor to suppress interferon regulatory factor 1-dependent
536 interferon-lambda and antiviral defense in airway epithelium. *Mucosal Immunol* 11: 958-967.
- 537 36. Selvaggi C, Pierangeli A, Fabiani M, Spano L, Nicolai A, et al. (2014) Interferon lambda 1-3 expression in
538 infants hospitalized for RSV or HRV associated bronchiolitis. *J Infect* 68: 467-477.
- 539 37. Spann KM, Tran KC, Chi B, Rabin RL, Collins PL (2004) Suppression of the induction of alpha, beta, and
540 lambda interferons by the NS1 and NS2 proteins of human respiratory syncytial virus in human
541 epithelial cells and macrophages [corrected]. *J Virol* 78: 4363-4369.
- 542 38. Brock SC, Goldenring JR, Crowe JE, Jr. (2003) Apical recycling systems regulate directional budding of
543 respiratory syncytial virus from polarized epithelial cells. *Proc Natl Acad Sci U S A* 100: 15143-
544 15148.
- 545 39. Utley TJ, Ducharme NA, Varthakavi V, Shepherd BE, Santangelo PJ, et al. (2008) Respiratory syncytial
546 virus uses a Vps4-independent budding mechanism controlled by Rab11-FIP2. *Proc Natl Acad Sci*
547 *U S A* 105: 10209-10214.
- 548 40. Barbieri MA, Li G, Mayorga LS, Stahl PD (1996) Characterization of Rab5:Q79L-stimulated endosome
549 fusion. *Arch Biochem Biophys* 326: 64-72.
- 550 41. Li G, Barbieri MA, Colombo MI, Stahl PD (1994) Structural features of the GTP-binding defective Rab5
551 mutants required for their inhibitory activity on endocytosis. *J Biol Chem* 269: 14631-14635.
- 552 42. Takeuchi R, Tsutsumi H, Osaki M, Sone S, Imai S, et al. (1998) Respiratory syncytial virus infection of
553 neonatal monocytes stimulates synthesis of interferon regulatory factor 1 and interleukin-1beta
554 (IL-1beta)-converting enzyme and secretion of IL-1beta. *J Virol* 72: 837-840.
- 555 43. Takeuchi R, Tsutsumi H, Osaki M, Sone S, Imai S, et al. (1998) Respiratory Syncytial Virus Infection of
556 Neonatal Monocytes Stimulates Synthesis of Interferon Regulatory Factor 1 and Interleukin-1 β
557 (IL-1 β)-Converting Enzyme and Secretion of IL-1 β . *J Virol* 72: 837-840.
- 558 44. Scagnolari C, Midulla F, Pierangeli A, Moretti C, Bonci E, et al. (2009) Gene expression of nucleic acid-
559 sensing pattern recognition receptors in children hospitalized for respiratory syncytial virus-
560 associated acute bronchiolitis. *Clin Vaccine Immunol* 16: 816-823.
- 561 45. Mordstein M, Neugebauer E, Ditt V, Jessen B, Rieger T, et al. (2010) Lambda Interferon Renders
562 Epithelial Cells of the Respiratory and Gastrointestinal Tracts Resistant to Viral Infections ∇ †. *J*
563 *Virol* 84: 5670-5677.
- 564 46. Nayak RC, Keshava S, Esmon CT, Pendurthi UR, Rao LV (2013) Rab GTPases regulate endothelial cell
565 protein C receptor-mediated endocytosis and trafficking of factor VIIa. *PLoS One* 8: e59304.
- 566 47. Johnson SM, McNally BA, Ioannidis I, Flano E, Teng MN, et al. (2015) Respiratory Syncytial Virus Uses
567 CX3CR1 as a Receptor on Primary Human Airway Epithelial Cultures. *PLoS Pathog* 11: e1005318.

- 568 48. Harcourt J, Alvarez R, Jones LP, Henderson C, Anderson LJ, et al. (2006) Respiratory syncytial virus G
569 protein and G protein CX3C motif adversely affect CX3CR1+ T cell responses. *J Immunol* 176:
570 1600-1608.
- 571 49. Tripp RA, Dakhama A, Jones LP, Barskey A, Gelfand EW, et al. (2003) The G glycoprotein of respiratory
572 syncytial virus depresses respiratory rates through the CX3C motif and substance P. *J Virol* 77:
573 6580-6584.
- 574 50. Currier MG, Lee S, Stobart CC, Hotard AL, Villenave R, et al. (2016) EGFR Interacts with the Fusion
575 Protein of Respiratory Syncytial Virus Strain 2-20 and Mediates Infection and Mucin Expression.
576 *PLoS Pathog* 12: e1005622.
- 577 51. Monick MM, Cameron K, Staber J, Powers LS, Yarovinsky TO, et al. (2005) Activation of the epidermal
578 growth factor receptor by respiratory syncytial virus results in increased inflammation and
579 delayed apoptosis. *J Biol Chem* 280: 2147-2158.
- 580 52. Kurt-Jones EA, Popova L, Kwinn L, Haynes LM, Jones LP, et al. (2000) Pattern recognition receptors
581 TLR4 and CD14 mediate response to respiratory syncytial virus. *Nat Immunol* 1: 398-401.
- 582 53. Marchant D, Singhera GK, Utokaparch S, Hackett TL, Boyd JH, et al. (2010) Toll-like receptor 4-
583 mediated activation of p38 mitogen-activated protein kinase is a determinant of respiratory virus
584 entry and tropism. *J Virol* 84: 11359-11373.
- 585 54. You Z, Fischer DC, Tong X, Hasenburger A, Aguilar-Cordova E, et al. (2001) Coxsackievirus-adenovirus
586 receptor expression in ovarian cancer cell lines is associated with increased adenovirus
587 transduction efficiency and transgene expression. *Cancer Gene Ther* 8: 168-175.
- 588 55. Tayyari F, Marchant D, Moraes TJ, Duan W, Mastrangelo P, et al. (2011) Identification of nucleolin as a
589 cellular receptor for human respiratory syncytial virus. *Nat Med* 17: 1132-1135.
- 590 56. Holguera J, Villar E, Munoz-Barroso I (2014) Identification of cellular proteins that interact with
591 Newcastle Disease Virus and human Respiratory Syncytial Virus by a two-dimensional virus
592 overlay protein binding assay (VOPBA). *Virus Res* 191: 138-142.
- 593 57. Donalisio M, Rusnati M, Cagno V, Civra A, Bugatti A, et al. (2012) Inhibition of human respiratory
594 syncytial virus infectivity by a dendrimeric heparan sulfate-binding peptide. *Antimicrob Agents
595 Chemother* 56: 5278-5288.
- 596 58. Kalinowski A, Ueki I, Min-Oo G, Ballon-Landa E, Knoff D, et al. (2014) EGFR activation suppresses
597 respiratory virus-induced IRF1-dependent CXCL10 production. *Am J Physiol Lung Cell Mol Physiol*
598 307: L186-196.
- 599 59. Barbieri MA, Roberts RL, Gumusboga A, Highfield H, Alvarez-Dominguez C, et al. (2000) Epidermal
600 Growth Factor and Membrane Trafficking. Egf Receptor Activation of Endocytosis Requires Rab5a
601 151: 539-550.
- 602 60. Chen PI, Kong C, Su X, Stahl PD (2009) Rab5 isoforms differentially regulate the trafficking and
603 degradation of epidermal growth factor receptors. *J Biol Chem* 284: 30328-30338.
- 604 61. Fukui K, Tamura S, Wada A, Kamada Y, Igura T, et al. (2007) Expression of Rab5a in hepatocellular
605 carcinoma: Possible involvement in epidermal growth factor signaling. *Hepatol Res* 37: 957-965.
- 606 62. Meng J, Stobart CC, Hotard AL, Moore ML (2014) An overview of respiratory syncytial virus. *PLoS
607 Pathog* 10: e1004016.
- 608 63. Yu D, Wei L, Zhengxiu L, Jian L, Lijia W, et al. (2010) Impact of bacterial colonization on the severity,

- 609 and accompanying airway inflammation, of virus-induced wheezing in children. Clin Microbiol
610 Infect 16: 1399-1404.
- 611 64. Gias E, Nielsen SU, Morgan LA, Toms GL (2008) Purification of human respiratory syncytial virus by
612 ultracentrifugation in iodixanol density gradient. J Virol Methods 147: 328-332.
- 613 65. Caillet M, Janvier K, Pelchen–Matthews A, Delcroix-Genête D, Camus G, et al. (2011) Rab7A Is
614 Required for Efficient Production of Infectious HIV-1. PLoS Pathog 7.
- 615 66. Deng Y, Chen W, Zang N, Li S, Luo Y, et al. (2011) The antiasthma effect of neonatal BCG vaccination
616 does not depend on the Th17/Th1 but IL-17/IFN-gamma balance in a BALB/c mouse asthma
617 model. J Clin Immunol 31: 419-429.
- 618 67. Mehedi M, McCarty T, Martin SE, Le Nouën C, Buehler E, et al. (2016) Actin-Related Protein 2 (ARP2)
619 and Virus-Induced Filopodia Facilitate Human Respiratory Syncytial Virus Spread. PLoS Pathog 12.

620

621

622

623

624

625

626

627

628

629

630 **Figure legends**

631 **FIGURE 1. Rab5a depletion reduces RSV propagation**

632 A549 cells were transfected with either siRNA control (siCon) or specific siRNAs targeting

633 Rab proteins (siRabs), and then were infected with RSV as described in Materials and
634 Methods. (A) Bright field image of infected cell cultures, taken at 36 h p.i. Bar = 20 μ m.
635 (B) Analysis of efficiency of Rab protein depletion. (C) RSV propagation was scored by
636 measuring the amount of RSV both in attached cells and released into the culture
637 supernatants by RT-qPCR. (D) The graph shows the comparative average size of RSV
638 syncytia with siRab1a (n=64), siRab2a (n=72), siRa4a (n=59), siRab5a (n=67), siRab6a
639 (n=70), siRab7a (n=52), siRab8a (n=61), siRab9a (n=59), siRab11a (n=57), relative to that
640 siCON (n=114) from 20 different fields using ImageJ. Bars represent the means \pm SD for
641 three independent experiments, each performed in duplicate. P values were calculated
642 based on unpaired Student's t-test between siCON and siRabs. Significant results (***,
643 $p < 0.001$, **, $p < 0.01$ and *, $p < 0.05$) are indicated.

644 **FIGURE 2. RSV increases Rab5a expression at early infection times.**

645 Nasopharyngeal aspirates (NPA) from 26 RSV-infected infants and 24 uninfected controls
646 were used and processed as described in Materials and Methods. Total protein was
647 extracted from the cell pellets. (A) Rab5a protein expression in NPAs. A549 cells were
648 infected with RSV and at indicated times (0, 1, 2, 6 12 h p.i.), samples were collected for
649 measurement of Rab5a mRNA and protein expression. (B) Rab5a mRNA and (C) protein
650 expression at various post-infection times. (D) Semi-quantitative analysis of the data from
651 (C), using Image J. Bars represent mean \pm SD for three independent experiments performed
652 in duplicate. P values were calculated based on unpaired Student's t-test between Control

653 and RSV infection. Significant results (***, $p < 0.001$, **, $p < 0.01$ and *, $p < 0.05$) are
654 indicated.

655 **FIGURE 3. Inactive Rab5a protein decreased RSV replication**

656 A549 cells were transiently transfected with GFP-expressing constructs of Rab5 WT, Rab5
657 Q79L (C/A), Rab5 S34N (D/N) for 24 h, then infected with RSV for 36 h. (A) The cells
658 were fixed and stained with anti-RSV (red) and anti-DAPI (blue) antibodies. Arrowheads
659 point to RSV and Rab5a co-localization. (B) Viral titers of cell culture homogenates were
660 quantified by plaque assay (plaque forming units, PFU) at 36 h p.i.. * $P < 0.05$; ** $P < 0.01$;
661 compared with control (RSV, transfected with vector only). Data are shown as mean \pm SD
662 of duplicates from at least three independent experiments in duplicate.

663 **FIGURE 4. Depletion of Rab5a exaggerates IFN- λ production**

664 Transfection of A549 cells with siRNA control (siCon), Rab5a siRNA, EGFP empty vector
665 (EV) or EGFP S34N, followed by infection with RSV as indicated, have been described in
666 Materials and Methods. All mRNAs were quantified by RT-qPCR, and IFN in the
667 supernatant was quantified by ELISA. (A) IFN- α ; (B) IFN- α (IFNA1) mRNA; (C) IFN- β ;
668 (D) IFN- β (IFNB1) mRNA; (E) IFN- λ ; (F) IFN- λ mRNA. Bars represent the mean \pm SD
669 for three independent experiments performed in duplicate. P values were calculated based
670 on Bonferroni of one-way analysis. ***, $p < 0.001$, **, $p < 0.01$ and *, $p < 0.05$ vs. CON and
671 RSV; ^^, $p < 0.01$ and ^, $p < 0.05$ vs. siCON and siRab5a.

672 **FIGURE 5. Depletion of Rab5a exaggerates IRF1 production**

673 Transfected with either siRNA control (siCon) or siRNAs targeting IRF1 protein (siIRF1)
674 for 24 h p.i. and infection with RSV have been described in Materials and Methods. (A)
675 IRF1 protein expression, detected by immunoblotting. (B). Semi-quantitative analysis from
676 (A), using Image J. (C) IRF1 protein expression using immunofluorescence assay. (D)
677 Semi-quantitative analysis (mean fluorescence intensity, MFI) from (C), using Image J.
678 Bars represent the mean \pm SD for three independent experiments performed in duplicate.
679 P values were calculated based on Bonferroni of one-way analysis. ***, $p < 0.001$ vs. CON
680 and RSV; ^^^, $p < 0.001$ vs. siCON and siRab5a.

681 **FIGURE 6. Rab5a mediates IFN- λ production via IRF1**

682 Transfection with siRNA control (siCon) or siRNAs targeting IRF1 protein (siIRF1), and
683 RSV infection, were conducted as described in Materials and Methods. (A) Knockdown
684 efficiency of IRF1 by specific siRNA, determined by immunoblotting. (B) IFN- λ
685 production in supernatants, using ELISA. Bars represent mean \pm SD for three independent
686 experiments performed in duplicate. P values were calculated based on Bonferroni of one-
687 way analysis. ***, $p < 0.001$, **, $p < 0.01$, vs. CON and RSV; ^^, $p < 0.01$ vs. siCON and
688 siIRF1 in (B). ***, $p < 0.001$, **, $p < 0.01$, vs. co-transfected with siRab5a and siIRF1 and
689 transfected with Rab5a or transfected with IRF1 in (C).

690

691 **FIGURE 7. Rab5a depletion activates JAK-STAT1 pathway**

692 siRNA transfection and RSV infection were performed as described in Materials and

693 Methods. (A) Total STAT1 and Phospho-STAT1 (Tyr701) protein expression by
694 immunoblotting. (B) Semi-quantitative analysis of total STAT1 from (A) with Image J. (C,
695 D) Semi-quantitative analysis of phospho-STAT1 α or phospho-STAT1 β from (A) with
696 Image J. (E) A549 cells were transfected with indicated siRNA, infected with RSV, and
697 treated with JAK1 inhibitor (Baricitinib, 5 nM) or STAT1 inhibitor (Fludarabine, 2.5 μ M)
698 for 24 h. Viral titers of cell culture homogenates were assessed by plaque assay as before.
699 Bars represent mean \pm SD for three independent experiments performed in duplicate. P
700 values were calculated based on Bonferroni of one-way analysis, ***, $p < 0.001$, **, $p < 0.01$,
701 vs. CON and RSV. P values were calculated based on unpaired Student's t-test, ^, $p < 0.01$
702 vs. siCON and siRab5a in (B, D). ^^, $p < 0.001$ vs. siRab5a and siRab5a with Baricitinib
703 or siRab5a with Fludarabine in (E).

704 **FIGURE 8. Rab5a depletion increases RIG-I and Mx1 mRNA expression**

705 Transfection of A549 cells and RSV infection were performed as before. (A, C) RIG-I and
706 Mx1 mRNA expression, measured by RT-qPCR. (B, D) Where indicated JAK1 inhibitor
707 (Baricitinib, 5 nM) or STAT1 inhibitor (Fludarabine, 2.5 μ M) were used for 24 h; RIG-I
708 and Mx1 mRNA were quantified by RT-qPCR. Bars represent mean \pm SD for three
709 independent experiments performed in duplicate. P values were calculated based on
710 Bonferroni of one-way analysis, ***, $p < 0.001$, **, $p < 0.01$, vs. CON and RSV. P values
711 were calculated based on unpaired Student's t-test, ^, $p < 0.01$ vs. siCON and siRab5a. ###,
712 $p < 0.001$, ##, $p < 0.01$ vs. siRab5a and siRab5a with Baricitinib or siRab5a with Fludarabine.

713 **FIGURE 9. Overview**

714 (A) RSV activates Rab5a that inactivates IRF1. IRF1 inactivation inhibits IFN- λ
715 production, which decreases JAK/STAT1 pathway activation, resulting in suppression of
716 host defense and increased viral replication. (B) Upon Rab5a depletion (by siRNA), IRF1-
717 induced IFN- λ is increased, which results in decreased viral titers.

718 **ACKNOWLEDGMENTS**

719 This research is supported by grants from the National Natural Science Foundation of
720 China 81670011, 91642107.

721

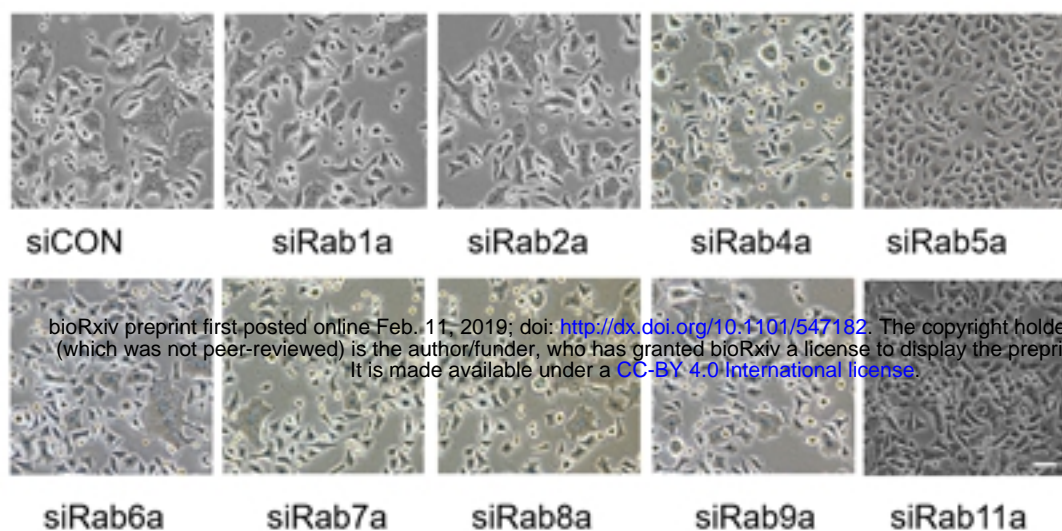
722

723

724

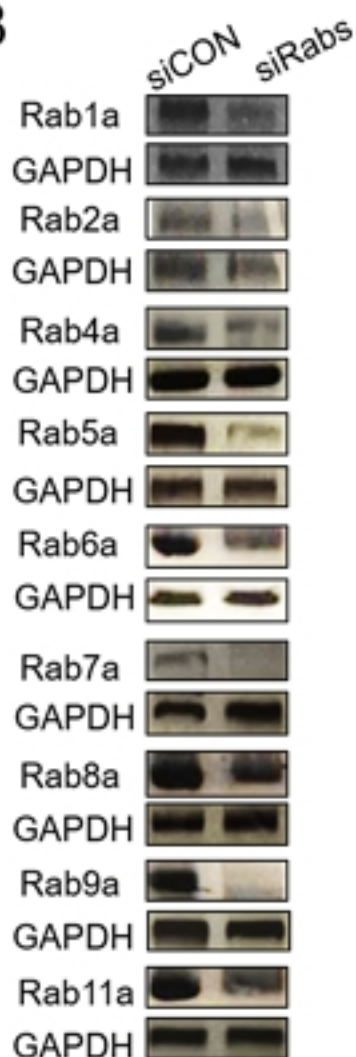
725

A

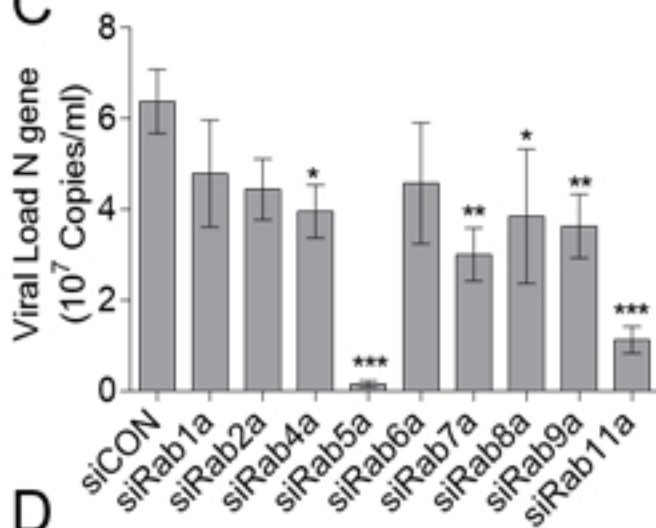


bioRxiv preprint first posted online Feb. 11, 2019; doi: <http://dx.doi.org/10.1101/547182>. The copyright holder for this preprint (which was not peer-reviewed) is the author/funder, who has granted bioRxiv a license to display the preprint in perpetuity. It is made available under a [CC-BY 4.0 International license](https://creativecommons.org/licenses/by/4.0/).

B



C



D

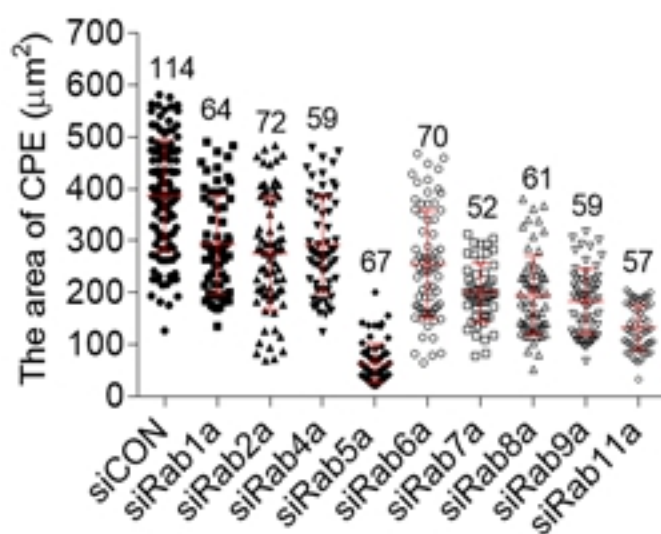


Figure 1

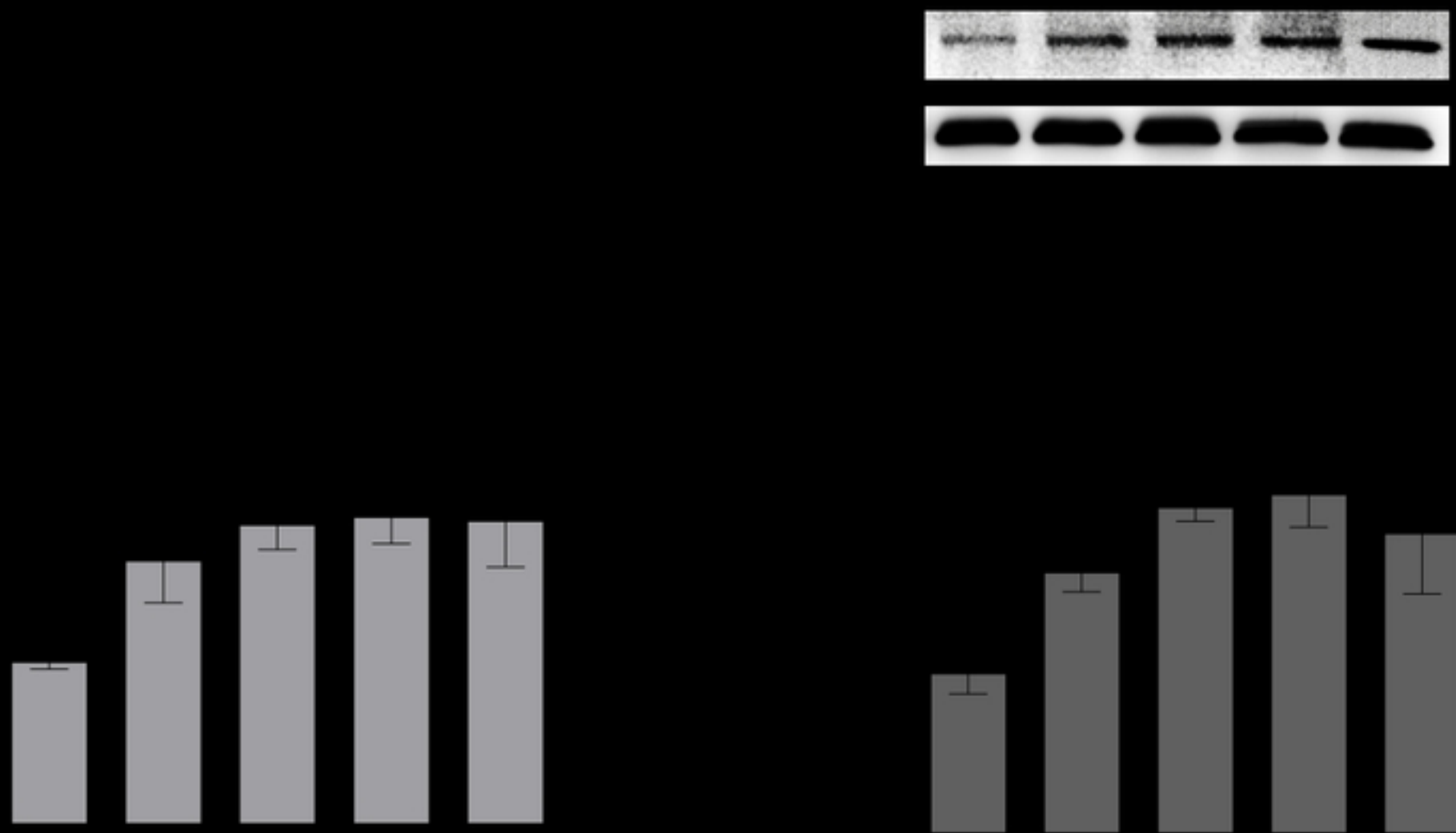


Figure2

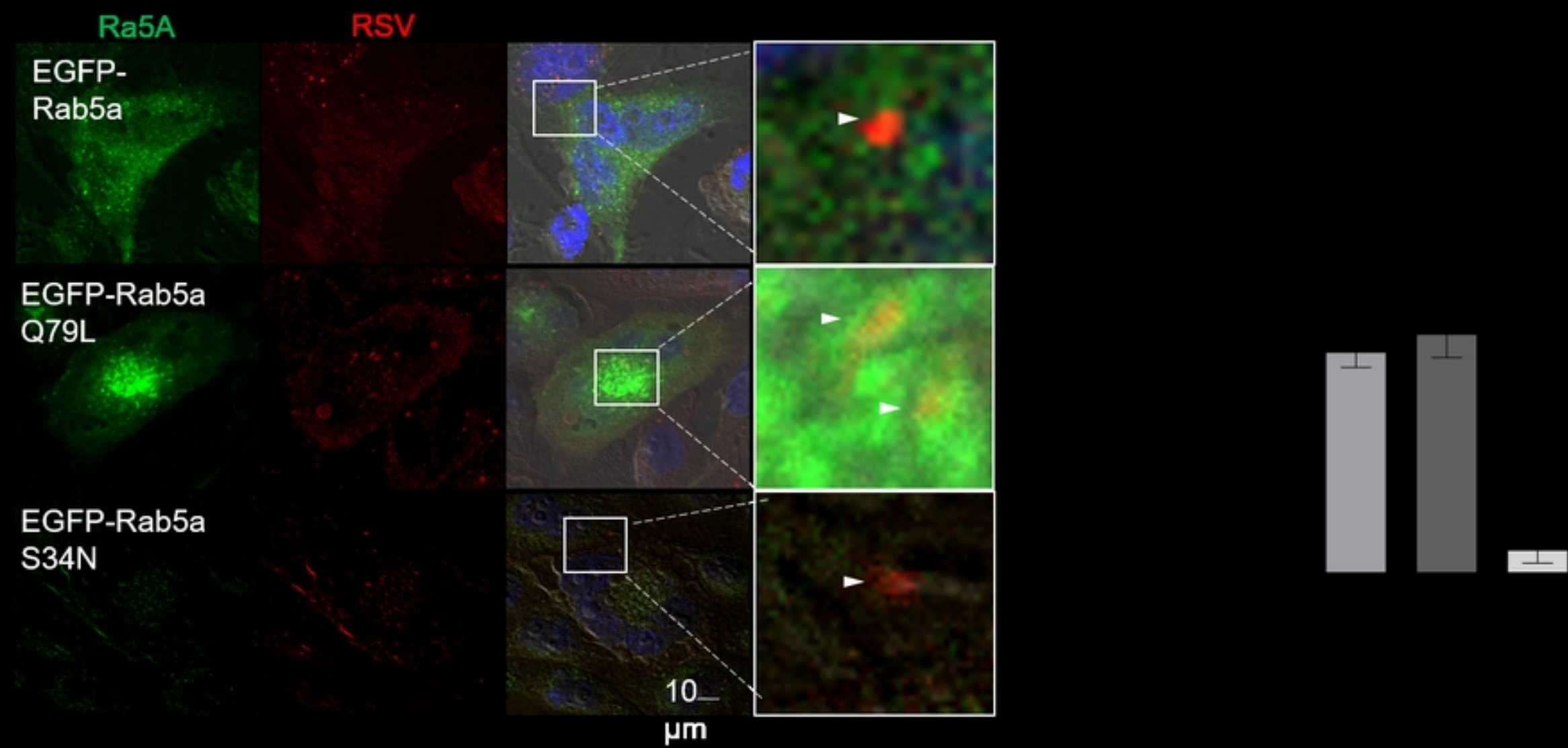


Figure3

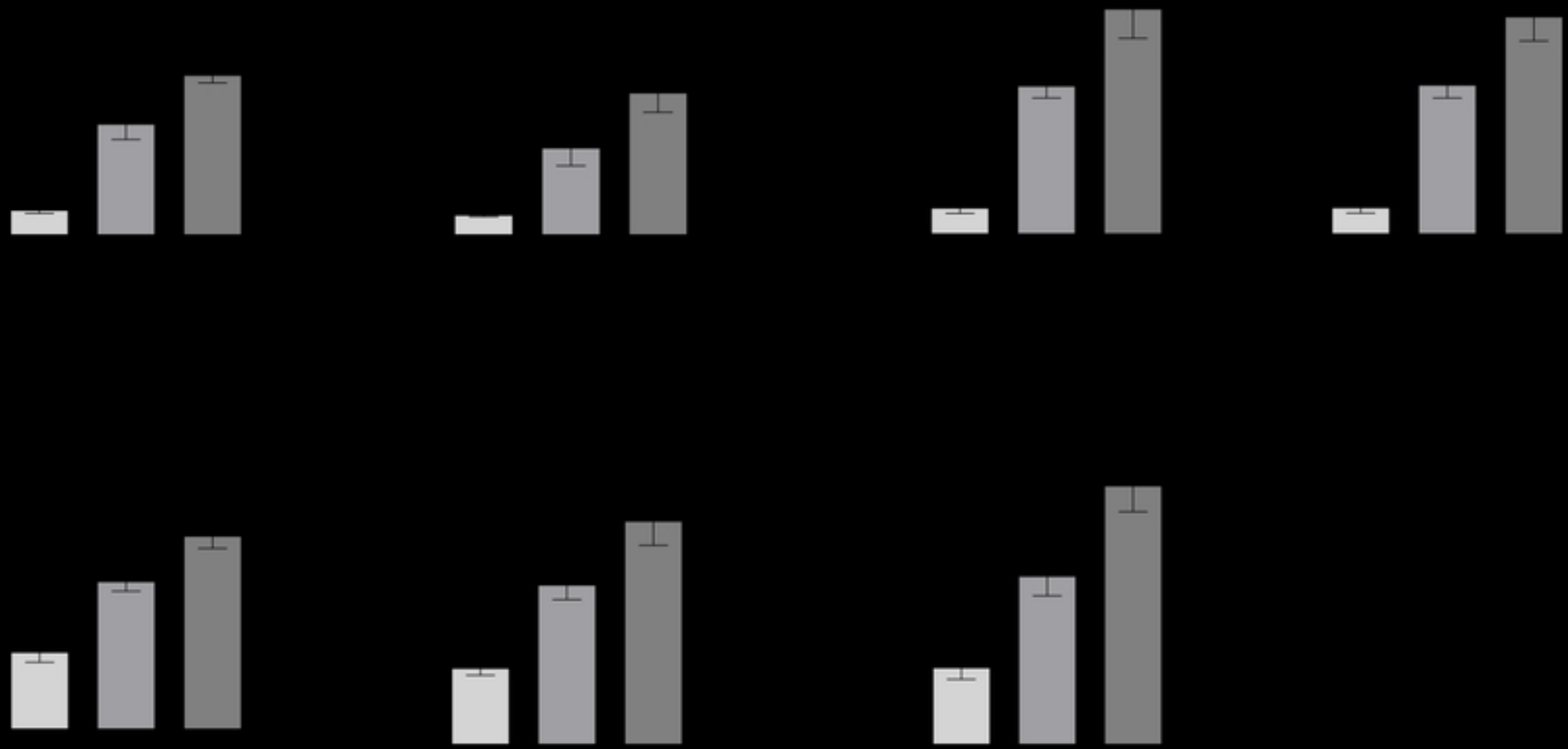


Figure4

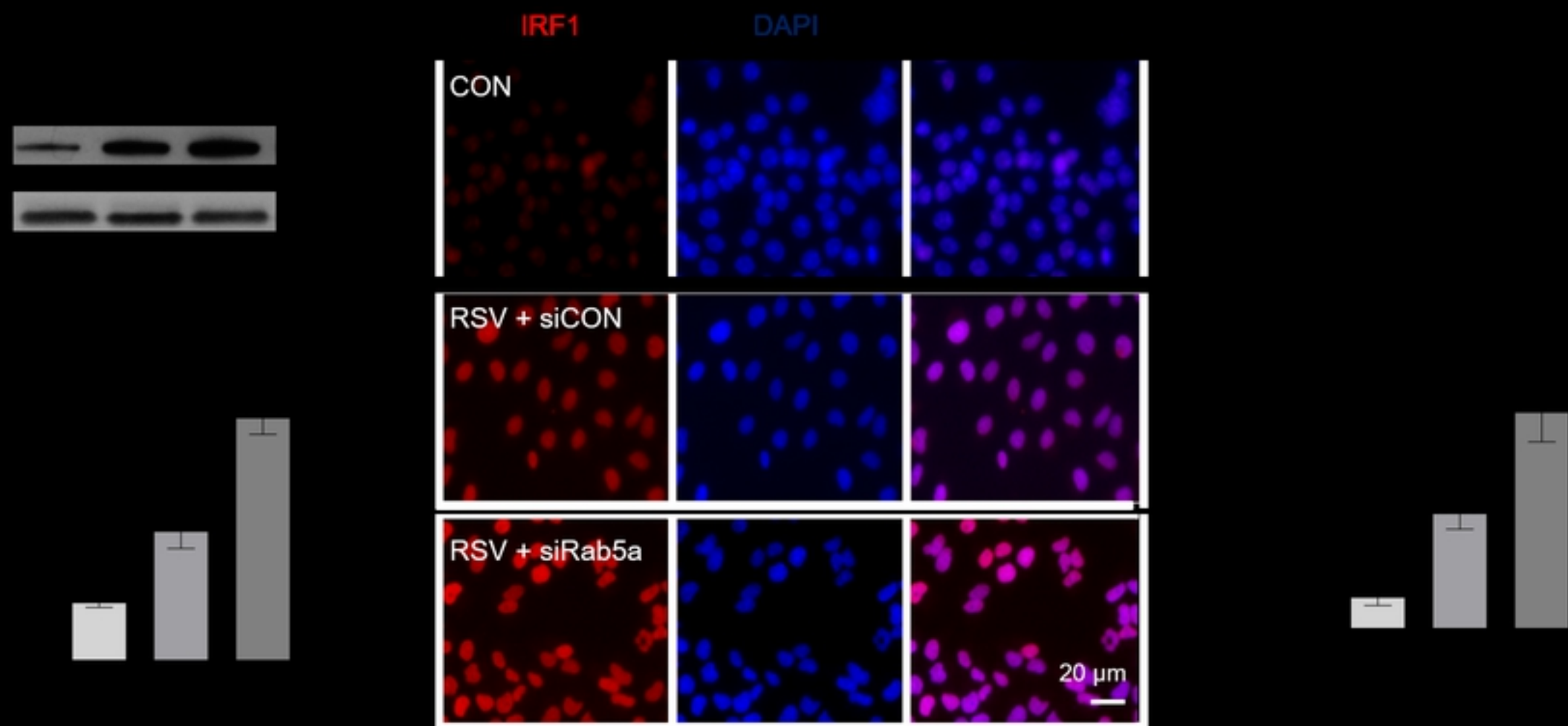


Figure 5

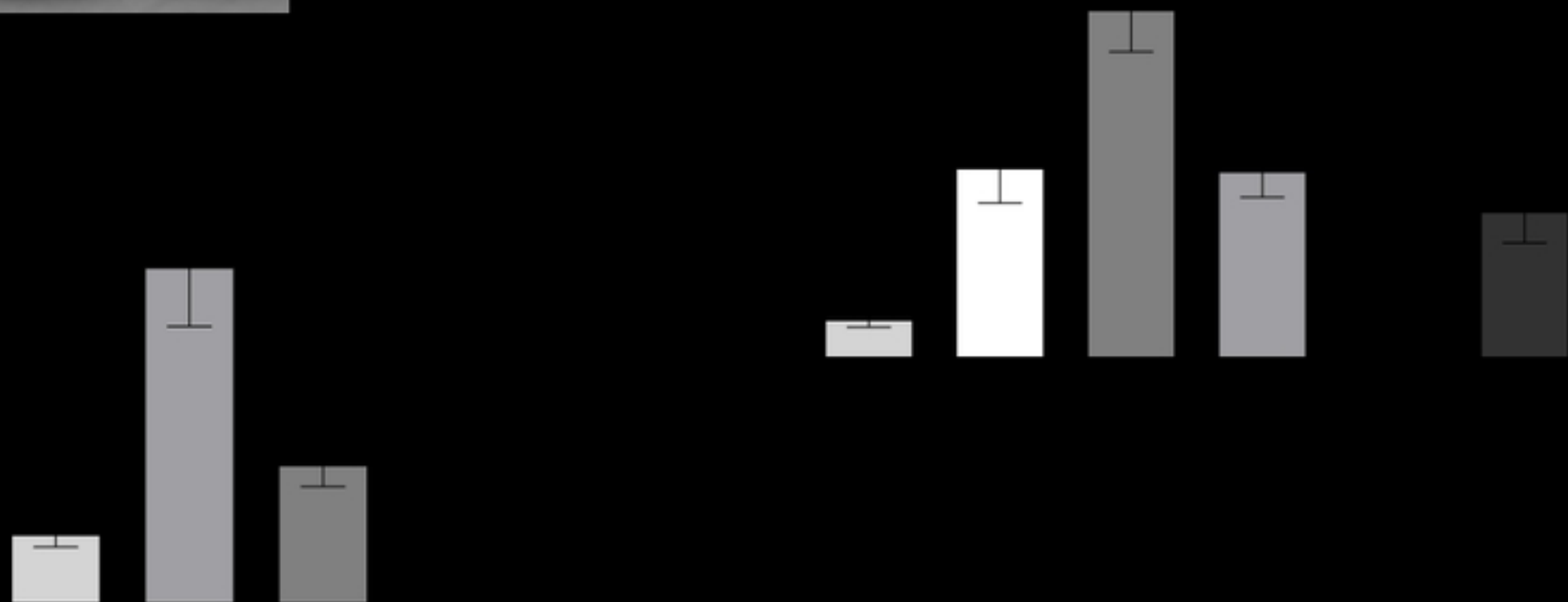


Figure6

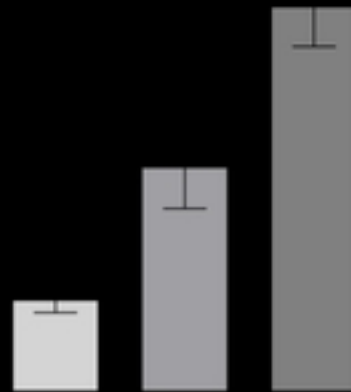
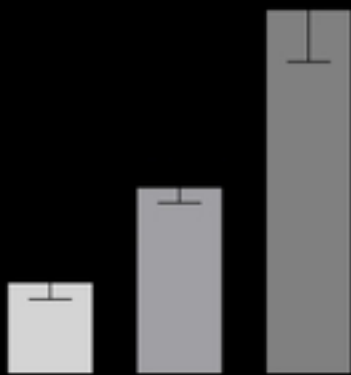
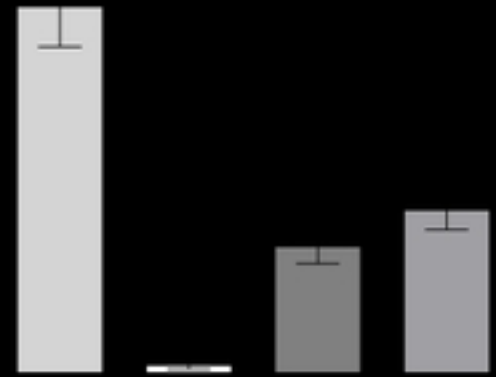
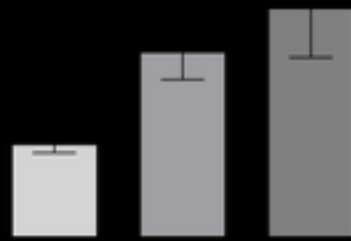
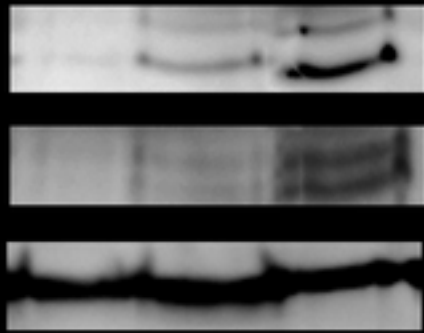


Figure 7

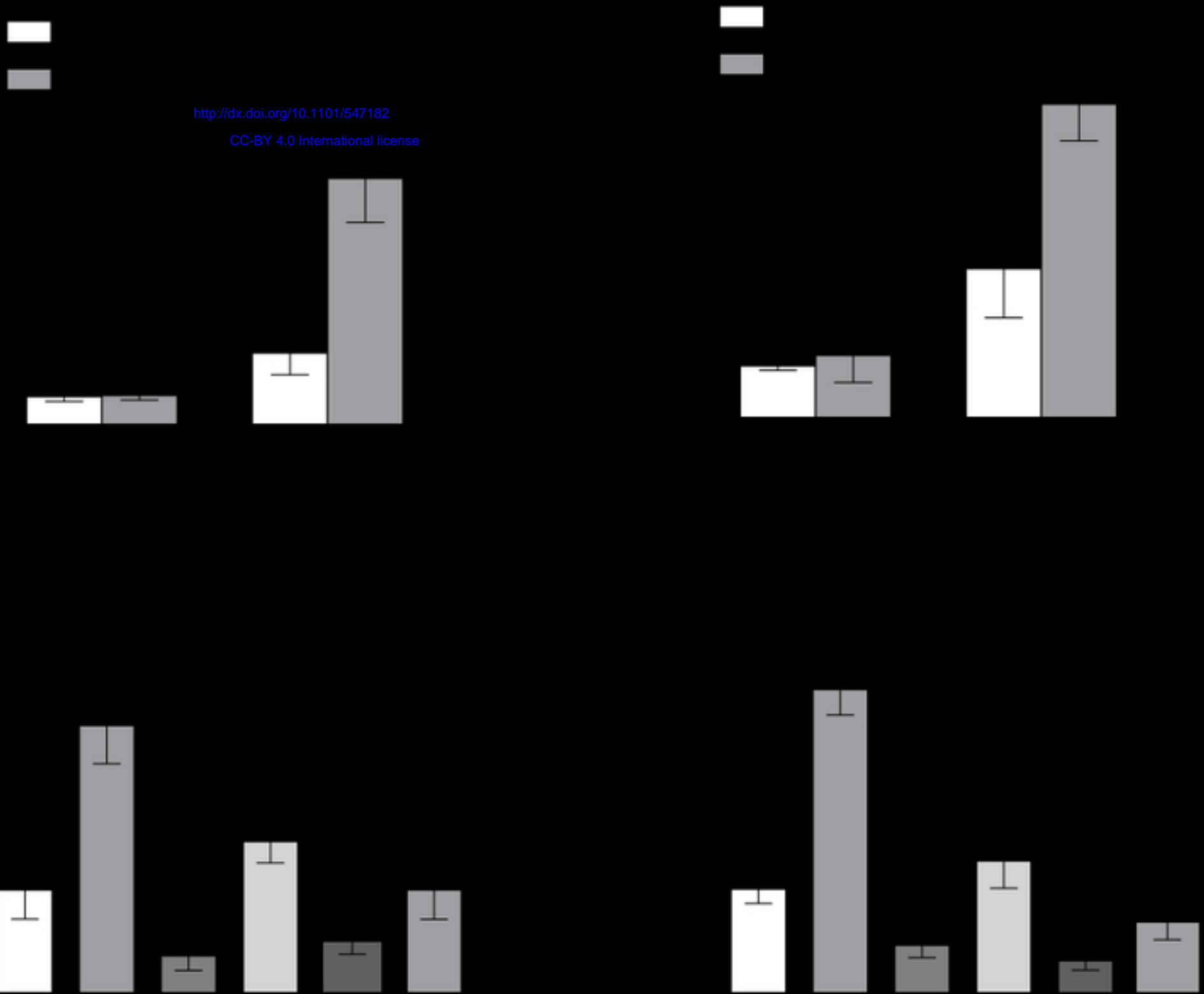


Figure8

